J. RADIAT. RES., 40, 169–181 (1999)

DS86 Neutron Dose : Monte Carlo Analysis for Depth Profile of ^{152}Eu Activity in a Large Stone Sample

SATORU ENDO[1]*, KAZUO IWATANI[2], TAKAMITSU OKA[3], MASAHARU HOSHI[1], KIYOSHI SHIZUMA[4], TETSUJI IMANAKA[5], JUN TAKADA[1], SHOICHIRO FUJITA[6] and HIROMI HASAI[7]

[1]Research Institute for Radiation Biology and Medicine, Hiroshima University, Hiroshima 734–8553, Japan
[2]Hiroshima Prefectural College of Health and Welfare, Mihara, Hiroshima 723–0053, Japan
[3]Kure University, Gohara, Kure 724–0792, Japan
[4]Faculty of Engineering, Hiroshima University, Kagamiyama, Higashi-Hiroshima 739–8527, Japan
[5]Research Reactor Institute, Kyoto University, Kumatori, Osaka 590–0494, Japan
[6]Radiation Effects Research Foundation, Hiroshima 732–0815, Japan
[7]Department of Electrical Engineering, Hiroshima-Denki Institute of Technology, Hiroshima 739–0321, Japan
(*Received, November 4, 1998*)
(*Revision received, April 30, 1999*)
(*Accepted, May 6, 1999*)

^{152}Eu activity/Monte Carlo N-Particle Transport Code (MCNP)/Depth profile/ Hiroshima atomic bomb/DS86

The depth profile of ^{152}Eu activity induced in a large granite stone pillar by Hiroshima atomic bomb neutrons was calculated by a Monte Carlo N-Particle Transport Code (MCNP). The pillar was on the Motoyasu Bridge, located at a distance of 132 m (WSW) from the hypocenter. It was a square column with a horizontal sectional size of 82.5 cm × 82.5 cm and height of 179 cm. Twenty-one cells from the north to south surface at the central height of the column were specified for the calculation and ^{152}Eu activities for each cell were calculated. The incident neutron spectrum was assumed to be the angular fluence data of the Dosimetry System 1986 (DS86). The angular dependence of the spectrum was taken into account by dividing the whole solid angle into twenty-six directions. The calculated depth profile of specific activity did not agree with the measured profile. A discrepancy was found in the absolute values at each depth with a mean multiplication factor of 0.58 and also in the shape of the relative profile. The results indicated that a reassessment of the neutron energy spectrum in DS86 is required for correct dose estimation.

*Corresponding author: TEL; 0824–24–7612, FAX; 0824–22–7192, e-mail; endos@ipc.hiroshima-u.ac.jp
Present address: Faculty of Engineering, Hiroshima University, Kagamiyama, Higashi-Hiroshima 739–8527, Japan

INTRODUCTION

Atomic bomb (A-bomb) radiation dose in Hiroshima and Nagasaki was revised in 1987 as the Dosimetry System 1986 (DS86)[1]. The epidemiological data for A-bomb survivors based on the DS86 have been reported by the Radiation Effects Research Foundation (RERF)[2].

Meanwhile, measurement of A-bomb-exposed materials has continued. Recent results have revealed discrepancies of induced activities for ^{152}Eu, ^{60}Co, ^{32}P and ^{36}Cl between measured and the DS86-calculated values. The neutron spectrum based on the DS86 is over-estimated within 0.7 km, and furthermore, under-estimated at the distance of 1 km from the hypocenter[3–11]. The discrepancies have been discussed intensively, and a modified neutron spectrum using a Crack Model proposed by Hoshi et al.[12,13], is able to reproduce well all of the measured activities of ^{152}Eu, ^{60}Co, ^{32}P and ^{36}Cl at a distance within 1 km. However, discrepancies still exist for longer distances from the hypocenter.

Activation data from the surface to the deep part of thick materials are expected to yield information on a wider neutron energy range. Several large stone samples in Hiroshima were chosen for our investigation. Activation data of ^{152}Eu from one of those samples, i.e, a large stone pillar on Motoyasu Bridge located at distance of 132 m (MSW) from the hypocenter, were reported by Hasai et al.[3] in 1987.

In this article, the depth profile of ^{152}Eu activity induced in the granite pillar by the Hiroshima A-bomb neutrons is calculated by means of a Monte Carlo N-Particle Transport Code[14] (MCNP) assuming the DS86 neutron energy spectrum surrounding the pillar. The validity of DS86 is discussed, comparing the calculated depth profile with the measured profile.

MATERIALS AND METHODS

The analysis procedure is summarized as follows: 1) neutron fluence in the area concerned, the "cells" in the pillar was determined, using a normalized neutron field; 2) ^{152}Eu specific activity in each cell was calculated, convoluting the production rate by the DS86 neutron fluence surrounding the pillar; 3) the calculated depth profile was compared with the measured depth profile.

Details are given in the text.

Geometry

Figure 1 (a) shows an overview of the epicenter, the hypocenter, and the location and shape of the pillar together with the coordinate system used in the calculation. The pillar was regarded as a square column with a horizontal sectional size of 82.5 cm × 82.5 cm and a height of 179 cm. The origin of the coordinate system was defined as the center of the column. As the subject of calculation, twenty one cells were put inside the column as shown in Fig. 1 (a), (b) and (c). Each cell (#1–#20) was 10 cm × 10 cm × 4 cm, except for cell (#11) which was 2.5 cm thick. Several simplifications of the actual shape of the pillar were used for this calculation. The following

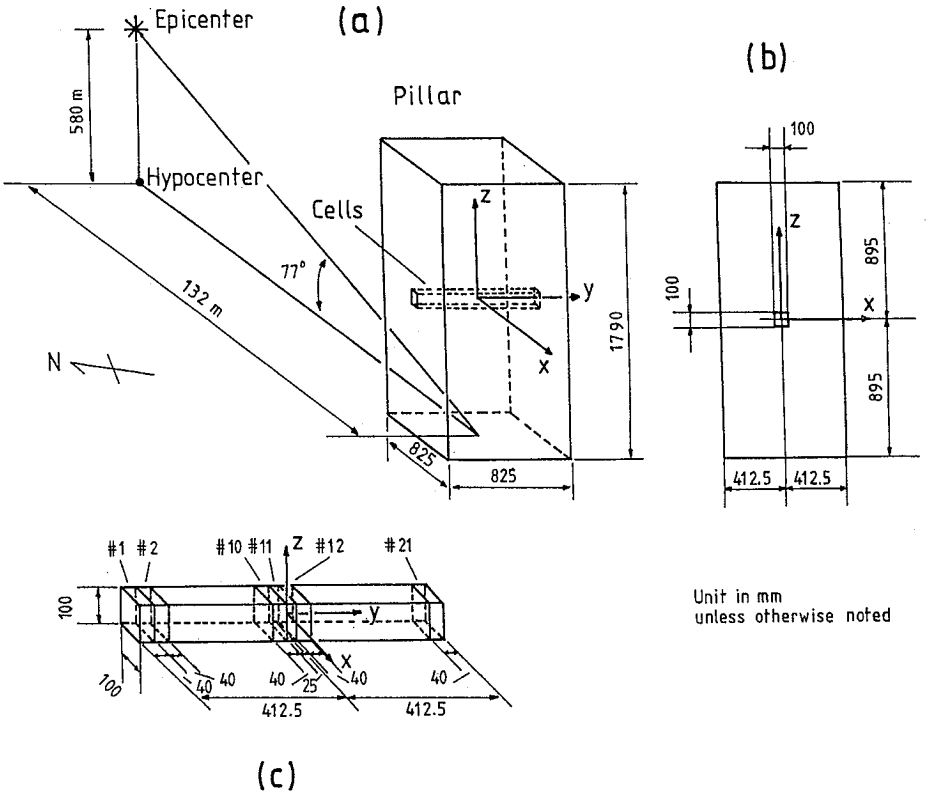

Figure 1. (a) Overview of the epicenter, hypocenter and the location and shape of the pillar, together with the coordinate system used in the calculation. (b) Side view of the pillar. (c) Size and numbering of the cells.

geometry was ignored; a box and a roof on the top of the pillar to accommodate an electric light, a vertical 3.5 cm diameter hole traversing the central part of the pillar to accommodate electric wires, small railings by the east and west sides of the pillar, and that the height of the sampling position is 1 cm lower than that of the calculated position . These contributions were presumed negligibly small to the main result.

Specific activity calculation

Specific activities A_k (Bq/mg) of ^{152}Eu produced in a cell (cell number k) are obtained by the decay constant of ^{152}Eu ($\lambda = 1.622 \times 10^{-9}$ s^{-1}) and numbers of ^{152}Eu atoms produced per mg of Eu in the cell k (N_k) as follows:

$$\begin{aligned} A_k &= \lambda N_k \\ &= \lambda n \int \phi_k(E)\sigma(E)\,dE, \end{aligned} \tag{1}$$

where n is a constant indicating numbers of ^{151}Eu atoms contained in 1 mg of natural Eu, $\phi_k(E)$ is neutron fluence in the cell k and $\sigma(E)$ is the ^{151}Eu(n, γ)^{152}Eu reaction cross section. The integration part of Eq. 1 (denoted by I) is expressed by the following equation when the incident neutron fluence coming into the pillar is given by angular fluence $\varphi(\Omega, E')$ for angle Ω and energy E',

$$I = \int \phi_k(E)\sigma(E)\,dE = \frac{1}{2\pi}\int\left[\int_{2\pi}\int \varphi(\Omega, E')\,q_k(\Omega, E, E')\,dE'\,d\Omega\right]\sigma(E)\,dE, \tag{2}$$

where $q_k(\Omega, E, E')dE'\,d\Omega\,dE$ is fluence of neutron with energy around E transported in the cell k divided by fluence of incident neutron with energy E' and solid angle Ω. In the calculation, the angle and energy were dealt with by dividing them into groups over the range of possible values. The angle Ω is divided into ℓ groups, energy E' into m groups and energy E into n groups. Equation 2 is expressed in the form of a summation as follows:

$$I = \sum_{N_A=1}^{\ell}\{\sum_{N_E=1}^{m} W(N_A)[\sum_{N_{E'}=1}^{n}\hat{\varphi}(N_A, N_{E'})\,\hat{q}_k(N_A, N_E, N_{E'})]\}\hat{\sigma}(N_E), \tag{3}$$

where N_A, N_E and $N_{E'}$ represent group numbers of Ω, E and E' respectively, $W(N_A)$ is the weight fraction (solid angle corresponding to group N_A divided by 2π), and $\hat{\varphi}$, $\hat{q}_k$, $\hat{\sigma}$ are functions in the summation form corresponding to φ, q_k, σ.

The formalism mentioned above is based on the following assumptions: (1) $\phi_k(E)$ in Eq. 1 is obtained by transporting neutrons emitted from the neutron source set at locations around the pillar. (2) The intensity of the neutron source is assumed as DS86 angular fluence. (3) The pillar material has no influence on the source intensity. (4) The angular distribution of the source intensity is taken into account by a convolution of neutron plane waves with different emitted angles.

MCNP calculation

The MCNP code (a Monte Carlo N-Particle Transport Code)[14] was used to calculate the quantity, $\hat{q}_k(N_A, N_E, N_{E'})$ in Eq. 3. This code was produced at Los Alamos National Laboratory and was obtained through the Nuclear Energy Data Center, Japan.

A plane wave source from a circular window, one of the standard sources included in the program, was used as the neutron source. Input specifications for the source were the coordinates of the center of the circular window, (x_0, y_0, z_0), the vector which represents the plane wave direction, (u, v, w), and the radius of the circular window. The total number of source windows was twenty-six and their specifications are shown in Table 1. Direction vectors were not necessarily normalized to an unit vector. The MCNP calculations were carried out for the q_k of the direction group I in the table. Considering the symmetrical arrangement of the cells, the values q_k for the direction groups II and III were obtained from the results of group I.

The F4 tally option of the MCNP code, i.e., the track length estimate, was chosen as the

estimator. This quantity corresponds to the mean fluence at the center of a cell of interest in units of $n \cdot cm^{-2}$. The q_k were the product of the calculated estimator and the area weight of the circular window.

The range of the tally energy E was from 1.0×10^{-11} MeV to 1.11 MeV and was divided into seventeen groups ($n = 17$). The energy boundaries of each group were the same as that for the DS86 angular fluence data as shown in Table 2.

Table 1. Source specifications.

Source Type	Center position of circular window			Plane wave direction I			II			III		
	x_0(cm)	y_0(cm)	z_0(cm)	u	v	w	u	v	w	u	v	w
1	0	−200	0	0	1	0	0	−1	0	±1	0	0
2	0	0	200	0	0	−1						
0	0	1										
3	0	−140	−140	0	1	−1	0	1	1	±1	0	±1
								0	−1	±1		
4	−140	−140	0	1	1	0	−1	1	0	±1	−1	0
5	−120	−120	120	1	1	−1	−1	±1	−1			
							1	±1	1			
							−1	±1	1			
							1	−1	−1			

Table 2. Energy groups for tally and $^{151}Eu(n, \gamma)^{152}Eu$ reaction cross section.

Group Number N_E'	Upper boundary of energy (MeV)	Cross section (barn)
1[a]	4.14×10^{-7}	5800
2	1.13×10^{-6}	2810
3	3.06×10^{-6}	235
4	1.07×10^{-5}	215
5	2.90×10^{-5}	177
6	1.01×10^{-4}	124
7	5.83×10^{-4}	49
8	1.23×10^{-3}	26
9	3.35×10^{-3}	15
10	1.03×10^{-2}	7.7
11	2.19×10^{-2}	4.6
12	2.48×10^{-2}	3.5
13	5.25×10^{-2}	2.4
14	1.11×10^{-1}	1.7
15	1.58×10^{-1}	1.4
16	5.50×10^{-1}	1.1
17	1.11×10^{0}	0.84

[a]The lowest boundary of energy is 1×10^{-11} MeV.

Table 3. Energy groups of incident neutrons.

Group No. N_E	Upper boundary of energy (MeV)
1[a]	4.14×10^{-7}
2	1×10^{-6}
3	1×10^{-5}
4	1×10^{-4}
5	1×10^{-3}
6	1×10^{-2}
7	1×10^{-1}
8	1×10^{0}

[a]The lowest boundary of energy is 1×10^{-11} MeV.

The energy spectrum of incident neutrons, $\varphi(W, E')$, was also divided into eight groups ($m = 8$) ranging from 1.0×10^{-11} MeV to 1.0 MeV, as shown in Table 3. In the thermal neutron region ($N_E = 1$), the energy distribution was given by the evaporation energy spectrum $p(E) \propto E \exp(-E/a)$, where a is a constant of 0.025 eV. In other energy regions, the source probability was set so that the neutron number per lethargy was uniform in each region.

The pillar was made of a solid piece of granite. The elemental composition data were taken from a previous article[3], and the cross section library used in the calculation was the same as that of another article[15]. These cross section data were continuous-energy data except for the manganese element, for which discrete-energy data were used. For the water content in the pillar, a ENDF/B[14] thermal treatment $S(\alpha, \beta)$[14] was applied.

Two types of benchmark test of the MCNP calculation were carried out with a ^{252}Cf neutron source and several moderators including a thick granite one. The results, published in two articles[15,16] verify the adequacy of the MCNP code for application to the calculation discussed here.

^{151}Eu(n, γ)^{152}Eu reaction cross section

The cross section for the ^{151}Eu(n, γ)^{152}Eu reaction used in the calculation is tabulated in Table 2. This is a cross section modified from that used by Hasai et al[3]. It was based on the Japanese evaluated nuclear data library[17] changing the intervals of energy groups and excluding the contribution from ^{151}Eu(n, γ) ^{152m2}Eu reaction.

Incident neutrons

The DS86 angular fluences were used as incident-neutron spectra $\varphi(N_A, N_{E'})$. We received this data on a magnetic tape from D. L. Preston in 1987[18]. The tape-package contained data for prompt and delayed neutrons, primary + secondary gamma rays and delayed gamma rays for Hiroshima and Nagasaki. The energy range of the prompt neutrons was from 1.0×10^{-11} MeV to 19.64 MeV and was divided into 37 groups. The delayed neutron data was divided into 23 groups ranging from 1.0×10^{-11} MeV to 4.72 MeV. A solid angle of 2π was divided into 240 ($N_A^* = 1 - 240$) angle groups only for the right hemi-sphere viewed from the hypocenter, considering symmetry in the x-z plane. There were data of 97 ground ranges (every 25 m from 100 to 2500 m) and

5 heights (1, 4, 9, 15 and 25 m). Angular fluence values in units of $n \cdot cm^{-2} \cdot W(N_A^*)^{-1}$ were given for each combination of city, ground range, energy group and height. The $W(N_A^*)$ is the weight fraction of angle group N_A^*, and proportional to its solid angle. The total value for all N_A^* is one. Since the weight fraction was zero for 40 out of 240 angle groups, data for 200 angle groups were used. The data used in the calculation were at a height of 1 m for Hiroshima. The fluence at the location of the pillar (at ground range 132 m (WSW)) was obtained by interpolating the data of ground ranges 125 and 150 m. The fluences for prompt and delayed neutrons were simply added up. The angle and energy group numbers were reduced to 26 and 8, respectively. Here, if direction vectors as shown in Table 1 are represented as $\Omega(i)$ (i = 1–26) and those of the DS86 data $\Omega^*(j)$ (j = 1–400) for 4π solid angle, the angle $\theta(i, j)$ between the i th and j th vector is calculated as follows.

$$\theta(i, j) = \cos^{-1} \frac{\Omega(i)\,\Omega^*(j)}{|\Omega(i)|\,|\Omega^*(j)|}. \tag{4}$$

Calculating this quantity for fixed j, changing i from 1 to 26, the i at minimum value $\theta(i, j)$ can be determined. If a function of $\mathrm{Min}^{-1}\{\theta(i, j)\}$ is defined as obtaining i at the minimum value $\theta(i, j)$, then the weight fraction and angular fluence of the i th group was expressed using the delta function ,which is $\delta(0) = 1$, and otherwise 0, as follows:

$$W(\Omega(i)) = \sum_{j=1}^{400} W(\Omega^*(j))\,\delta(i - \mathrm{Min}^{-1}\{\theta(i, j)\}). \tag{5a}$$

$$\varphi(\Omega(i)) = 1 / W(\Omega(i)) \sum_{j=1}^{400} W(\Omega^*(j))\,\varphi(\Omega^*(j))\,\delta(i - \mathrm{Min}^{-1}\{\theta(i, j)\}). \tag{5b}$$

Carrying out this procedure for all j, 400 angle groups were converted to 26 angle groups using each weight fraction.

As for energy groups, the 17 groups of the DS86 data in the range from 1.0×10^{-11} MeV to 1.0 MeV were reduced to 8 groups, assuming that the spectrum per lethargy in each energy group is uniform.

Figure 2 shows three examples of neutron energy spectra at 132 m ground range and 1 m height. The vertical axis represents total fluence per lethargy integrated for all angles. The thin solid line histogram is for the DS86 fluence with original energy groups. The thick solid line histogram shows the fluence of the reduced energy groups where the upper limit of energy is 1 MeV. It can be seen that the latter approximates well the former, except in the thermal region. Total scalar fluence was 2.267×10^{13} cm^{-2}. Because partial scalar fluence with energy upward of 1 MeV corresponded to 0.8%, and its contribution was ignored in the latter spectrum. The dashed line histogram is described below.

Influence of the river (the Motoyasu River) on the spectrum was checked with an air-over-

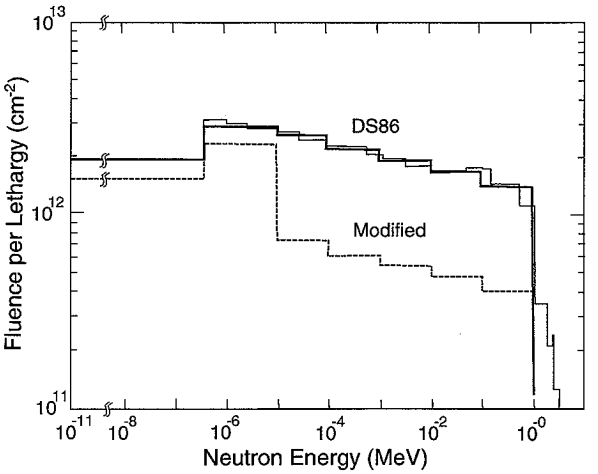

Figure 2. Neutron energy spectra at the location of the pillar. Thin solid line histogram indicates original energy-grouped fluence of DS86. Thick solid line histogram indicates reduced energy-grouped fluence used in the calculation. Dashed line histogram is an example of fluence modification to enable the calculated depth profile of ^{152}Eu activity to reproduce the measured one.

ground transport calculation, which was also carried out using the MCNP code. The air-over-ground geometries were represented by a circular cylinder, the lower portion composed of the ground, and the upper portion composed of the air, with the source in the air on the axis of the cylinder. Source height was 580 m, and the neutron spectrum of a point source was taken from the DS86 source term found in Table 1 in the DS86 report (Whalen)[1]. The composition and density data of air and ground were taken from Table 6 and Table 7 in the same report (Kerr et al.)[18].

The outer geometrical boundary of the atmosphere was defined by a cylinder having a radius of 3 km and a height of 2 km. The ground was defined by a 5.9 m thick cylinder having a radius of 3 km.

The river was located between 100 m and 140 m from the hypocenter in a concentric configuration. The river bottom level and surface level were 5.9 m and 3.9 m below the ground level. Output of the calculation was the neutron fluence in a zone over the river extending from the ground level to a height of 2 m. The number of energy groups was 10, adding the 9th 1–5 MeV group and the 10th 5–12 MeV group to the eight groups in Table 3. Angular distribution was not taken into account.

In calculated results, total fluence when the river was included in the geometry was lower by 8% compared with when it was not included. But the difference of the ratios of thermal neutron fluence to total fluence in the above two cases was 2%. That for the fluence in the energy region below 10 eV was 1.5%. Statistical error of MCNP calculations was estimated to be less than 1%. Accordingly, influences of the river on the incident neutron spectrum were confirmed to be negligible.

RESULTS AND DISCUSSION

Neutron attenuation in the stone

An example of calculated ^{152}Eu production rate is shown in Fig. 3. The plots indicate the partial production rate for four energy groups ($N_E = 1, 2, 5, 8$), where source location number is 1 and incident neutrons are specified by plane wave direction $(u, v, w) = (0, 1, 0)$. This figure shows typical neutron attenuations in the stone. Thermal neutrons ($N_E = 1$) attenuate exponentially with a diffusion length of about 10.6 cm. High energy neutrons ($N_E = 8$) decrease their energy gradually along their path in the stone material, and produce much ^{152}Eu inside the stone. The ^{152}Eu production rate of this energy group is lower than that of thermal neutrons at the incident surface,

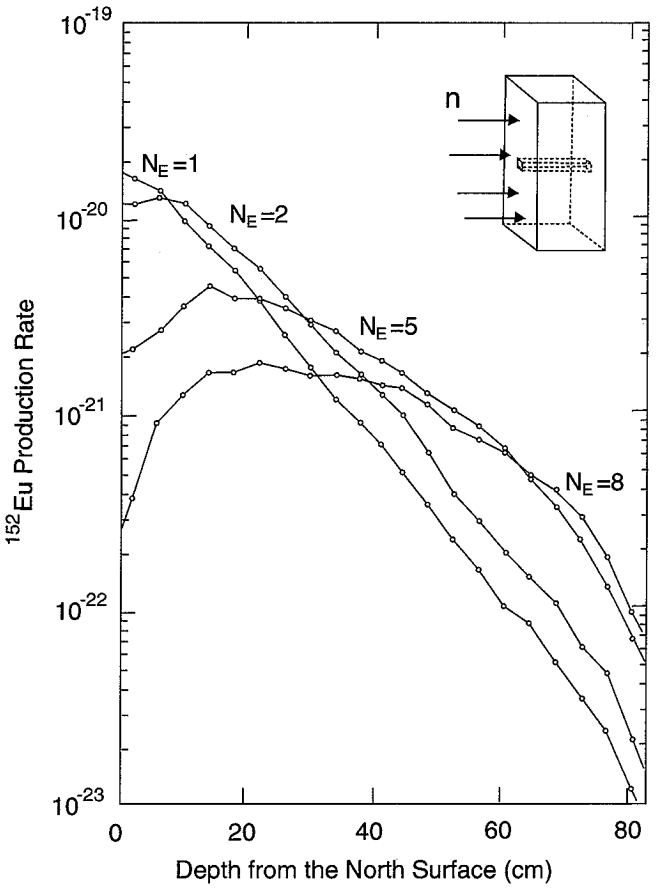

Figure 3. An example of calculated ^{152}Eu production rate as a function of depth. Each depth point represents the cell's center position. Source neutrons are incoming normally to the north surface of the pillar. The four curves show the incident energy dependence of ^{152}Eu production.

while two times higher at the deepest position (center of the stone). Thus it is seen that the contribution of high energy neutrons is prominent at the deepest position and the ^{152}Eu depth profile provides a certain amount of information on the incident neutron spectrum.

Depth profiles of ^{152}Eu specific activity

Superposing ^{152}Eu production by all energy and angle groups in each cell and multiplying by the λ value in Eq. 1, the depth profile of ^{152}Eu specific activity at the time of the bombing was obtained as shown by the open circle plot A in Fig. 4. Calculation uncertainty was within 1.2% for each cell point. The solid line is for eye guide. The histogram B in the figure is the measured profile that was modified from the original profile with 40 measuring points to a profile with 20 measuring points.

Calculated depth profile was higher with respect to absolute values and shallower in relative shape than the measured one. Ratios of specific activity at the deepest cell (#11) to that at the surface cell (#1) are 0.46 and 0.30 for the calculated and measured profiles, respectively. The mean ratio of measured specific activity to calculated activity for all cells is 0.58. The curve C in

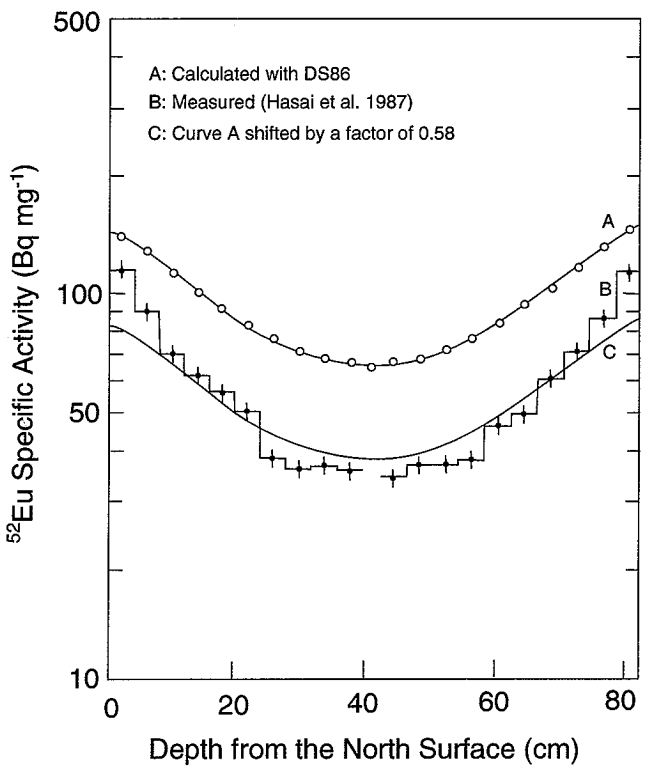

Figure 4. Calculated and measured depth profiles of ^{152}Eu specific activity (ATB). Curve C is added to facilitate comparison.

the figure shows the calculated profile multiplied by a factor of 0.58. As a result, the calculated profile based on DS86 fluence data does not reproduce the profile in detail though it can reproduce the measured depth profile of ^{152}Eu by a factor of about 2.

We confirmed these calculation results by using a Two Dimensional Discrete Originates Radiation Transport Code System (DOT) (calculation not shown). The magnitude of the factor is consistent with the Crack Model which assumed that the neutron spectrum is a summation of 95% of the DS86 spectrum and 5% of bare fission not changing the total neutron fluence, proposed by Hoshi et al.[12,13]. But, the profile was not reproduced. We also tested how much hydrogen content is needed to reproduce the measured depth profile. A calculation using a hydrogen content of 0.08% reproduced the measured shape (but not magnitude), however this value differed from measured ones (0.05%).

Modified incident neutron spectrum

Because of the difficulty of obtaining, with the unfolding technique, an incident neutron spectrum which would fit the measured depth profile, we attempted to apply some modified spectra to fit the profile. Figure 5 shows several comparisons of the calculated and measured profiles. Curve D in the figure indicates the depth profile assuming that all the incident neutrons have thermal energy. Total fluence was normalized to 62% of the DS86 value (2.267×10^{13} cm^{-2}). This is too deep to fit the measured profile, indicating that the measured profile included much information for epithermal and higher energy neutrons.

The three curves E, F and G in the figure indicate the depth profiles of specific activity when applying modified DS86 fluences. Here, the spectrum was modified from the DS86 one so that the incident fluence above a certain energy boundary E_b decreased to one half of the original data and the reduced amount of fluence was allotted to the lower energy part. The E_b values for the curve E, F and G were 1×10^{-6}, 1×10^{-5} and 1×10^{-4} MeV, respectively. The normalization factors for fitting the calculated profile to the measured one were 0.59, 0.57 and 0.56 for the curves E, F and G, respectively. Compared with the original curve C in Fig. 4, these curves tend to agree with the measured distribution. Curve F reproduces the profile within the errors of measured values particularly well. In the DS86 neutron fluence data, the rate of the fluence for energy above 1×10^{-5} MeV to total fluence is 43.2%. In curve F, the rate is one half of this, i.e., 21.6%. Corresponding to that, fluence for the energy below 1×10^{-5} MeV increases from 56.8% to 78.4% by a factor of 1.38. Total fluence for this curve corresponds to 1.29×10^{13} cm^{-2} . The spectrum used in the calculation of curve F, which was first given for each angle and then integrated for all angles, is shown by a dashed line in Fig. 2.

This analysis of the ^{152}Eu specific activity in the large stone pillar suggests that the DS86 fluence data should be examined further, e.g., with regard to evaluation for the total yields, epicenter height, casing and leaning of the bomb as well as the air-over-ground transport calculation.

In conclusion, the depth profile of the ^{152}Eu activity induced in a granite stone pillar by the Hiroshima Atomic-bomb neutrons was calculated by means of the MCNP code. The pillar was on the Motoyasu Bridge, located at a distance of 132 m (WSW) from the hypocenter. The neu-

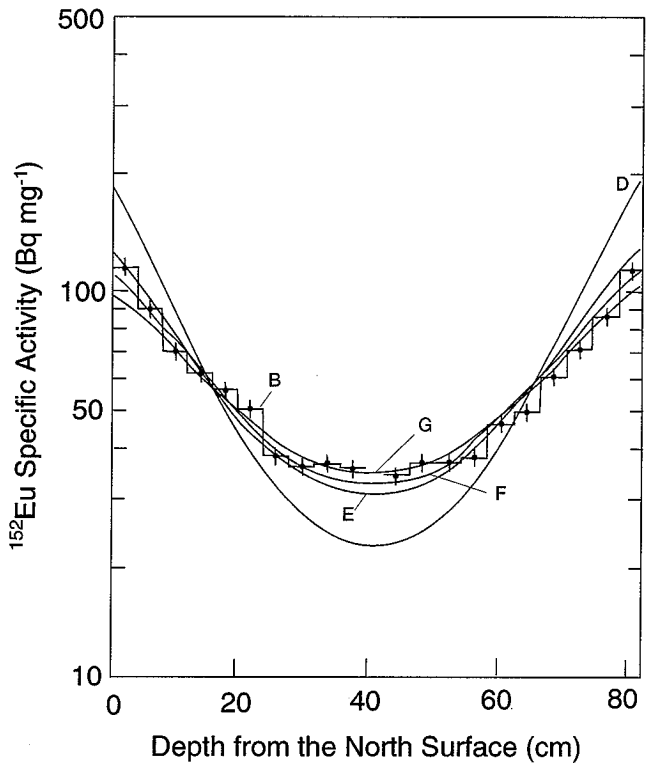

Figure 5. Depth profile of ^{152}Eu specific activity (ATB) when the incident neutron spectrum was modified (Curves D, E, F and G). Curve F reproduces the measured profile (Histogram B) within the error of measured values. See the text for details.

tron fluence derived at this location from the Dosimetry System 1986 was assumed as that incident to the pillar. The calculated depth profile of specific activity did not agree with the measured profile. Discrepancies were found in the absolute values at each depth with a mean multiplication factor of 0. 58 and also in the shape of the depth profiles. The results indicate that a reassessment of the neutron energy spectrum in the DS86 is required for correct dose estimation.

ACKNOWLEDGEMENTS

The authors appreciate the assistance and advice of Dr. Hiroyuki Hashikura of the Nuclear Engineering Research Laboratory, University of Tokyo, for installing the MCNP code. They thank Dr. Toshiso Kosako of the same laboratory for his help in the planning of this work. This study was supported by grants from the Matsuda Foundation and the Mitsubishi Foundation and by the Huge-Calculation Application Project of the Institute for Nuclear Study, University of Tokyo.

REFERENCES

1. Whalen, P. P. (1987) Calculation and verification of source terms. In: US-Japan Joint Reassessment of Atomic Bomb Radiation Dosimetry in Hiroshima and Nagasaki, Final report. Vol. 1, Ed. W. C. Roesh, The Radiation Effects Research Foundation, Hiroshima.
2. Preston, D. L. and Pierce, D. A. (1987) The effect of changes in dosimetry on cancer mortality risk estimates in the atomic bomb survivors. Report RERF TR 9–87, The Radiation Effects Research Foundation, Hiroshima.
3. Hasai, H., Iwatani, K.,, Shizuma, K., Hoshi, M., Yokoro, K., Sawada, S., Kosako, T. and Morishima, H. (1987) Europium-152 depth profile of a stone bridge pillar exposed to the Hiroshima atomic bomb: ^{152}Eu activities for analysis of the neutron spectrum. Health Phys. **53**: 227–239.
4. Hoshi, M., Hasai, H. and Yokoro, K. (1991) Studies of radioactivity produced by Hiroshima atomic bomb: 1. Neutron-induced radioactivity measurement for dose evaluation, J. Radiat. Res. **32**, Suppl. 2: 20–31.
5. Hoshi, M., Yokoro, K., Sawada, S., Shizuma, K., Hasai, H., Oka, T., Morishima, H. and Brenner, D. J. (1989) Europium-152 activity induced by Hiroshima atomic bomb neutrons: Comparison with the ^{32}P, ^{60}Co and ^{152}Eu activities in Dosimetry System 1986 (DS86). Health Phys. **57**: 831–837.
6. Shimizu, Y., Kato, H., Schull, W. J., Preston, D. L., Fujita, S. and Pierce, D. A. (1987) Life Span Study Report 11, Part 1. Comparison of risk coefficients for site-specific cancer mortality based on the DS68 and T65DR shielded kerma and organ doses. Report RERF TR 12–87, The Radiation Effects Research Foundation, Hiroshima.
7. Nakanishi, T., Ohtani, H., Mizuochi, R., Miyake, K., Yamamoto, T., Kobayashi, K. and Imanaka, T. J. (1991) Residual neutron-induced radionuclides in samples exposed to the nuclear explosion over Hiroshima: Comparison of the values with the calculated values. J. Radiat. Res. **32**, Suppl. 2: 69–82.
8. Straume, T., Egbert, S. D., Woolson, W. A., Finkel, R. C., Kubik, P. W., Gove, H. E., Sharma, P. and Hoshi, M. (1992) Neutron discrepancies in the New (DS86) Hiroshima Dosimetry. Health Phys. **63**: 421–426.
9. Shizuma, K., Iwatani, K., Hasai, H., Oka, T., Morishima, H. and Hoshi, M. (1992) Specific activities of ^{60}Co and ^{152}Eu in Samples collected from the atomic-bomb dome in Hiroshima. J. Radiat. Res. **33**: 151–162.
10. Shizuma, K., Iwatani, K., Hasai, H., Oka, T. and Morishima, H. (1993) Residual ^{152}Eu and ^{60}Co activities induced by neutron from the Hiroshima atomic bomb. Health Phys. **65**: 272–282.
11. Nakanishi, T., Miwa, K. and Ohki, R. (1998) Specific radioactivity of Europium-152 in roof tiles exposed to atomic bomb radiation in Nagasaki. J. Radiat. Res. **39**: 243–250.
12. Hoshi, M., Takada, J., Endo, S., Shizuma, K., Iwatani, K., Oka, T., Fujita, S. and Hasai, H. (1998) Problems of radiation dose evaluation in Hiroshima and Nagasaki, and their explanation. Radiat. Prot. Dos. **77**: 15–23.
13. Hoshi, M., Takada, J., Oka, T., Iwatani, K., Shizuma, K. and Hasai, H. (1996) A possible explanation for the DS86 discrepancy between the data and calculation in Hiroshima. Proceedings of the Nagasaki Symposium Radiation and Human Health: pp. 175–191, Elsevier Science B. V., Amsterdam.
14. Briesmeister, J.F. (Ed), (1993) MCNP-A General Monte Carlo N-Particle Transport Code Version 4A, Los Alamos National Laboratory (Los Alamos, NM, USA) Report LA-12625-M.
15. Hoshi, M., Hiraoka, M., Hayakawa, N., Sawada, S., Munaka, M., Kuramoto, A., Oka, T., Iwatani, K., Shizuma, K., Hasai, H. and Kobayashi, T. (1992) Benchmark test of transport calculations of gold and nickel activation with implications for neutron kerma at Hiroshima. Health Phys. **63**: 532–542.
16. Iwatani, K., Hoshi, M., Shizuma, K., Hiraoka, M., Hayakawa, N., Oka, T. and Hasai, H. (1994) Benchmark test of neutron transport calculations: II. Indium, nickel, gold, europium and cobalt activation with and without energy moderated fission neutrons by iron simulating the Hiroshima A-bomb casing. Health Phys. **67**: 358–366.
17. Aoki, T., Iijima, S., Kawai, M., Kikuchi, Y., Matsunobu, H., Nakagawa, T., Nakajima, Y., Nishigori, T., Sasaki, M., Watanabe, T., Yoshida, T. and Zukeran, A. (1986) Evaluation of FP cross sections for JENDLE-2. Proc. Int. Conf. on Nuclear Data for Basic and Applied Science, 2: 1627, Gordon & Breach Science Publisher, Glasgow.
18. Kerr, G. D., Pace, III, J. V., Mendelsohn, E., Loewe, W. E., Kaul, D. C., Dolatshahi, F., Egbert, S. D., Gritzner, M., Scott, Jr., W. H., Marcum, J., Kosako, T. and Kanda, K. (1987) Transport of initial radiations in air over ground. In: US-Japan Joint Reassessment of Atomic Bomb Radiation Dosimetry in Hiroshima and Nagasaki, Final report. Vol. 1, Ed. W. C. Roesh, The Radiation Effects Research Foundation, Hiroshima.